This is the Accepted Manuscript version of a Published Work that appeared in final form in International Journal of Biological Macromolecules 106 : 523-531(2018). To access the final edited and published work see https://doi.org/10.1016/j.ijbiomac.2017.08.043
© 2017. This manuscript version is made available under the CC-BY-NC-ND 4.0 license https://creativecommons.org/licenses/by-nc-nd/4.0/

# Chicken feathers as a natural source of sulphur to develop sustainable protein films with enhanced properties

**Tania Garrido[a], Itsaso Leceta[b], Koro de la Caba[a], Pedro Guerrero[a*]**
[a]BIOMAT research group, Department of Chemical and Environmental Engineering, Engineering College of Gipuzkoa, Plaza de Europa 1, 20018 Donostia-San Sebastián, Spain.

[b]BIOMAT research group, Department of Applied Mathematics, Engineering College of Gipuzkoa, Plaza de Europa 1, 20018 Donostia-San Sebastián, Spain.

*Corresponding author. Tel +34 943018535

E-mail address: pedromanuel.guerrero@ehu.eus

## Abstract

In this work, the effect of hydrolyzed keratin on the properties of soy protein-based films was analyzed when different manufacture processes were employed. It is widely known that the processing method selected can affect the film properties as a function of the structure obtained during the film formation. Therefore, the assessment of hydrolyzed keratin/soy protein films processed by casting and compression moulding was carried out by means of the analysis of physicochemical, thermal, mechanical, optical and surface properties. It was observed that the incorporation of hydrolyzed keratin, obtained from a simpler, environmentally friendlier and more sustainable extraction method, resulted in the improvement of the thermal stability of the films, irrespective of the processing method employed. Moreover, the films processed by compression moulding showed enhanced tensile strength, which increased with the incorporation of hydrolyzed keratin due to the formation of disulfide bonds.

**Keywords:** agro-industrial waste; sustainability; protein film.

## 1. Introduction

The research of new applications and alternative sources of biopolymers has experienced a huge increase in the last years, mostly due to the growing interest in the economical valorisation of agro-industrial wastes and by-products as well as their environmentally friendly management [1-3]. In fact, a huge amount of agricultural waste is produced every year, but the vast majority is underutilization; thus, a great opportunity to valorise it and reduce its environmental impact is missed [4]. Interestingly, the studies in this field are becoming more and more frequent. Bhatnagar et al. [5] valorised the solid waste product from oil industry and employed it as an adsorbent for water pollution; Liu et al. [6] used the sunflower head residue as a reinforcement in polymeric materials; Uranga et al. [7] studied the employment of fish gelatin, which is obtained from fish processing waste, as packaging films; and Xu et al. [8] employed grape pomace, obtained from juice or winemaking, as antimicrobial agent. The above mentioned works are some recent examples of the potential of industrial wastes and by-products to obtain raw materials and increase resource efficiency.

Chicken feathers, waste from the poultry industry, are considered a critical problem in many countries due to their limited applications [9]. Indeed, feathers are commonly burned or buried, even disposed as a total waste in landfills, causing environmental problems [10]. Therefore, the employment of chicken feathers as a source of raw materials for applications such as packaging, tissue engineering, water purification, or fuel storage could be an alternative [11-14]. It is well known that feathers are mainly composed of a structural protein, keratin (> 90%), rich in hydrophobic residues and cysteine, which promotes crosslinking by disulphide bonds [15]. The high content of cysteine turns keratin into a potential source of sulphur, which could promote interactions by disulphide bonds, enhancing the film stability. Although

S-S bonds provide strength and stiffness to the keratin in the solid state, they can be an impediment during the film processing in solution since they cause the insolubility of keratin [16]; hence, feather keratin must be pre-treated. Physical and chemical treatments have been reported [17]. Physical treatments involve high temperature (80-140 °C) and/or high pressure steam (70-100 kPa) to hydrolyze feathers. Additionally, chemical treatments used acids or alkalis at the boiling temperature for over 2-3 h. In this work, the application of high temperatures was avoided in order to use an inexpensive, simple and environmentally friendly method to obtain hydrolyzed keratin by a more sustainable manner. It was observed that the addition of sodium hydroxide as a reducing agent was effective in breaking disulphide bonds and, therefore, peptides and free amino acids were obtained, which meant the solubilisation of keratin. The hydrolyzed keratin (HK) solution was employed along with soy protein isolate (SPI) to develop fully renewable films.

Soy protein, a by-product from soy oil production, can be purified to obtain soy protein isolate. This protein has been widely used as an alternative to petroleum-derived polymers due to its attractive properties, such as renewability, abundance and biodegradability [18]. Soy protein fractions can be classified in four categories by its sedimentation rate in fractional ultracentrifugation: 2S, 7S, 11S and 15S. Among these four protein fractions, 7S (β-conclycinin) and 11S (glycinin) represent more than 80% and the 7S/11S ratio is estimated to be around 0.5-1.3 [19]. β-Conclycinin has a molecular weight of 180 kDa and disulfide bonds are not present in its structure; unlike glycinin, which has a molecular weight of 320-350 kDa and a total of 20 disulfide bonds [20]. However, the hydrolyzed keratin has around 11% of cysteine and 4-fold sulphur content than SPI, so that the incorporation of hydrolyzed keratin into soy protein isolate solution can promote the formation of disulfide bonds and enhance the

film properties. In this work, SPI/HK films were processed by solution casting and compression moulding. Overall, the processing of films is based on three main steps. Firstly, chemical agents and/or processing conditions break the intramolecular interactions among polymeric chains. Afterwards, these chains are rearranged and, finally, a new three dimensional network is formed by intermolecular interactions among the components of the film forming formulation. These three steps are involved in both casting and compression moulding methods; however, the last step differs from one technique to the other, since the protein chains have more time to rearrange in the solution casting method and, thus, the final properties can change [21, 22]. Hence, the employment of different processing methods allows to tailor the film properties as a function of the properties required for a specific application [23].

In view of the above, solution casting and compression moulding processes were employed in this research work to manufacture SPI/HK films and the effect of each processing method on film properties was analyzed. Moreover, the behaviour of the films with different HK contents was assessed by the analysis of physicochemical, thermal, mechanical, optical and surface properties.

## 2. Materials and methods

### 2.1 Materials

Soy protein isolate (SPI), with a minimum of 90% protein content on dry basis, was obtained from ADM Protein Specialties Division, Netherlands. SPI contains a maximum of 5% moisture, 4% fat, 5% ash and its isoelectric point is 4.6. Chicken feathers were kindly supplied by Lumagorri S.L. Glycerol, supplied by Panreac, was used as plasticizer.

## 2.2 Preparation of hydrolyzed keratin (HK)

Chicken feathers were washed with water and dried at room temperature. Then, the quills and the barbs were cut into small pieces and grinded. Afterwards, the grinded feathers were treated in a Soxhlet device with methanol during 3 h and then, they were dried. Pre-treated chicken feathers (CF) were mixed with NaOH (1 M) in a CF/NaOH ratio of 1:20 (w/v) and the mixture was stirred during 8 h at room temperature. After that, 100 mL of distilled water were added and the solution was filtered. In order to determine the sulphur content in HK solution, elemental analysis was carried out using an Euro EA Elemental Analyzer (EuroVecto, Italy). The determined sulphur content was 4.2%.

## 2.3 Preparation of films

Films were prepared by solution casting (wet method, W) or compression moulding (dry method, D). SPI film forming solution was prepared by dissolving 5 g of SPI in 100 mL of HK solution prepared as described above. The concentration of CF in HK solutions was fixed at 3, 6 or 9 wt % (based on SPI dry basis). The pH was appropriately adjusted to 10 before heating the dispersion at 80 ºC for 30 min under magnetic stirring. After that, 30 wt % glycerol (based on SPI dry basis) was added and the solution was maintained at the same temperature for 30 min. On one hand, the solution was poured into Petri dishes, dried at room temperature and films were peeled from the dishes. These films were designated as HK0-W (control sample for solution casting), HK3-W, HK6-W and HK9-W. On the other hand, the solution was freeze-dried using an Alpha 1-4 LD freeze dryer. The powder obtained was thermally compacted by applying a pressure of 12 MPa for 2 min, using a caver laboratory press, previously heated up to 150 ºC. The films were designated as HK0-D (control sample

for compression moulding), HK3-D, HK6-D and HK9-D. All films were conditioned in an ACS Sunrise 700 V controlled bio-chamber at 25 ºC and 50% relative humidity for 48 h prior to testing.

### 2.4 Characterization of films

#### 2.4.1 Moisture content (MC), water uptake (WU) and total soluble matter (TSM)

Three square-shaped samples of each film were weighed ($m_w$) and dried in an air-circulating oven at 105 ºC for 24 h. After that time, the films were reweighed ($m_0$) and the MC was determined by the following equation:

$$\text{MC}\ (\%) = \frac{m_W - m_0}{m_W} \times 100 \quad (1)$$

Then, samples were completely immersed in 70 mL of distilled water at room temperature. After 1-8 and 24 h, the samples were removed from water, wiped, weighed ($m_t$) and immersed again into water. The WU of each film was calculated as:

$$\text{WU}\ (\%) = \frac{m_t - m_0}{m_0} \times 100 \quad (2)$$

Afterwards, specimens were dried in an air-circulating oven at 105 °C for 24 h and weighed ($m_f$). TSM was expressed as the percentage of film dry matter solubilised after 24 h of immersion in distilled water [24]:

$$\text{TSM}\ (\%) = \frac{m_0 - m_f}{m_0} \times 100 \quad (3)$$

#### 2.4.2 Water vapour permeability (WVP)

Water vapour permeability (WVP) was analyzed in a controlled humidity environment chamber PERME™ W3/0120 according to ASTM E96-00 [25]. Circles of 7.40 cm diameter and a test area of 33 $cm^2$ were cut for each sample. The set up was subjected to a temperature and a relative humidity of 38 ºC and 90%, respectively. Water vapour transmission rate (WVTR) was calculated by the following expression:

$$WVTR\left(\frac{g}{s\ cm^2}\right)=\frac{G}{t\times A} \quad (4)$$

where G is the change in weight (g), t is time (s), and A is the test area ($cm^2$). WVP was calculated as:

$$WVP\left(\frac{g}{cm\ s\ Pa}\right)=\frac{WVTR\times L}{\Delta P} \quad (5)$$

where L is the thickness of the test specimen (cm) and ΔP is the partial pressure difference of the water vapour across the film (Pa). WVP was calculated and reported for three specimens of each sample.

### 2.4.3 Water contact angle (WCA)

Water contact angle measurements were performed at room temperature with a Neurtek contact angle meter model Oca20 Dataphysiscs Instruments. A film sample was laid on a movable sample stage and about 3 μL of distilled water were placed onto the film surface to estimate the hydrophobic character. The contact angle images were recorded at 0, 5 and 10 min after dropping the water on the sample, using SCA20 software. Five replicates were made per formulation.

### 2.4.4 Colour measurements

Colour was analyzed with a colourimeter CR-400 Croma Meter, Konica-Minolta. Films were placed on the surface of a white standard plate (calibration plate values $L^*= 97.39$, $a^*= 0.03$ and $b^*= 1.77$) and $L^*$, $a^*$ and $b^*$ colour parameters were measured using the CIELab scale: $L^*= 0$ (black) to $L^*= 100$ (white), $-a^*$(greenness) to $+a^*$(redness) and $-b^*$(blueness) to $+b^*$(yellowness). Ten replicates were made per formulation and the colour difference ($\Delta E^*$), referred to the control film, was calculated by the following equation:

$$\Delta E^* = \sqrt{(\Delta L^*)^2 + (\Delta a^*)^2 + (\Delta b^*)^2} \quad (6)$$

### 2.4.5 Transparency (T)

A spectrophotometer V-630 UV-Jasco was employed to determine the transparency (T) of the film. T was calculated by the following equation:

$$T = \frac{A_{600}}{L} \quad (7)$$

where $A_{600}$ is the absorbance at 600 nm and L is the films thickness (mm). Three specimens were tested for each composition.

### 2.4.6 Differential scanning calorimetry (DSC)

Differential scanning calorimetry (DSC) measurements were performed on a Mettler Toledo DSC 822. Samples of around 4 mg were subjected to a heating ramp from -50 ºC to 225 ºC at a rate of 10 ºC/min under nitrogen atmosphere to avoid oxidative reactions. Sealed aluminium pans were used to prevent mass loss during the experiment.

### 2.4.7 Thermogravimetric analysis (TGA)

Thermogravimetric analysis (TGA) was performed using a Mettler Toledo SDTA 851 equipment. Experiments were carried out in a temperature range from 25 ºC to 800 ºC at a constant rate of 10 ºC/min under nitrogen atmosphere to avoid thermo-oxidative reactions.

### 2.4.8 Tensile testing

Tensile strength (TS), elongation at break (EB) and elastic modulus (EM) were measured according to ASTM D638-03 standard [26], using a MTS Insight 10 electromechanical testing system. Samples were cut into strips of 4.75 mm × 22.25 mm and the crosshead rate was 1 mm/min. Five specimens were tested for each composition.

### 2.4.9 Dynamic mechanical analysis (DMA)

Thermo-mechanical measurements were performed using a DMA Explexor 100 N, Gabo Qualimeter. Experiments were performed in a temperature range from -100 ºC to 120 ºC at a heating rate of 2 ºC/min. The measurements were carried out under tension at a constant frequency of 1 Hz and the strain applied was fixed at 0.05%.

### 2.4.10 X-ray photoelectron spectroscopy (XPS)

XPS was performed in a SPECS spectrometer using a monochromatic radiation equipped with Al Kα (1486.6 eV). The binding energy was calibrated by Ag $3d_{5/2}$ peak at 368.28 eV. All spectra were recorded at 90 º take-off angle. Survey spectra were recorded with 1.0 eV step and 40 eV analyser pass energy and the high resolution regions with 0.1 eV step and 20 eV pass energy. All core level spectra were referenced to the C 1s neutral carbon peak at 284.6 eV. Spectra were analysed using the CasaXPS

2.3.16 software, and peak areas were quantified with a Gaussian–Lorentzian fitting procedure.

### 2.4.11 Gloss measurements

Gloss was analyzed at 60 º incidence angle according to the ASTM D523-14 [27] using a Konica-Minolta Multi Gloss 268 plus gloss meter. Measurements were taken ten times for each sample.

### 2.4.12 Scanning electron microscopy (SEM)

The morphology of the film surface was visualized using a Hitachi S-4800 scanning electron microscopy. Samples were mounted on a metal stub with double-side adhesive tape and coated under vacuum with gold, using JEOL fine-coat ion sputter JFC-1100 in an argon atmosphere prior to observation. All samples were examined using an accelerating voltage of 15 kV.

### 2.4.13 Statistical analysis

Data were subjected to one-way analysis of variant (ANOVA) by means of a SPSS computer program (SPSS Statistic 23.0). Post-hoc multiple comparisons were determined by the Duncan's test with the level of significance set at $P < 0.05$.

## 3. Results and discussion

### 3.1 Physical properties

The study of the behaviour of the films in presence of water can provide information about the film integrity and stability in humid environments. Therefore, properties such as moisture content (MC), total soluble matter (TSM), water vapour

permeability (WVP), water uptake (WU) and water contact angle (WCA) were analyzed. Firstly, MC, TSM and WVP values are presented in **Table 1**. As known, moisture content is important as far as it can act as a plasticizer in the polymeric matrix. As can be observed, moisture content values were higher for the films processed by casting. However, these values showed no significant difference ($P > 0.05$) when hydrolyzed keratin was incorporated. Regarding TSM, an upward trend was followed for the films processed by both methods, and the values increased with HK addition. This trend may be due to the presence of free amino acids or low molecular weight peptides that are not connected by covalent crosslinkages with other film components. Therefore, the rise in HK content resulted in an increase of the film solubility. In relation to WVP, an improvement was observed when solution casting was employed. This improvement could be due to the reorganization of protein chains since a longer drying period is provided when the wet process is used. Concerning HK incorporation, WVP values did not change significantly ($P > 0.05$) in HK-W films; however, the addition of HK into HK-D formulations resulted in the increase of the water vapour permeability.

The water resistance can be expressed in terms of water uptake. WU is related to the diffusion process in which small molecules are transported randomly from one side to the other, which is influenced by crosslinking, molecular interactions, crystallinity, as well as the presence of fillers in the film [28]. For all films, the rate of water absorption was fast in the first hour and then, the equilibrium was reached after few hours (**Fig. 1**). In the case of HK-W films, the WU values started to decrease within 24 h of immersion due to the beginning of the film disintegration. In contrast, the films processed by compression moulding maintained the water uptake values constant after 24 h, indicating the major stability of these films. Furthermore, it was observed that the

incorporation of hydrolyzed keratin affected the uptake capacity, allowing a higher water uptake, obtaining 2-fold values when 9 wt % HK was added.

The knowledge of the hydrophobicity of the films allows for the detection of changes in the orientation of hydrophobic groups toward the surface, caused by changes in the molecular structure of the protein upon denaturation [29]. The hydrophilic or hydrophobic character of the films was evaluated by measuring the water contact angle on the film surface as a function of time and the values are displayed in **Fig. 2**. Overall, WCA values higher than 90 º correspond to a hydrophobic character or low wettability of films [30]. In this instance, the films processed by casting showed higher values than those processed by compression and HK0-W films showed values around 90 º, confirming their hydrophobicity. This behaviour can be attributed to a lower concentration of polar groups toward the surface because of a longer period of time for the interactions between the blend components in the case of processing by casting. On the other hand, the hydrophilic character of the films was promoted by the addition of hydrolyzed keratin due to the incorporation of the hydrophilic amino acids present in HK. Furthermore, WCA values decreased with time, indicating the wettability of the films.

Regarding optical properties, colour and transparency of the SPI-based films were assessed and the results are displayed in **Table 2**. The films processed by casting had higher $L^*$ values, resulting in brighter films. However, the addition of HK darkened the films significantly ($P < 0.05$) to the detriment of lightness in comparison to the control film. An opposite trend was found for $a^*$ and $b^*$ parameters. In fact, it was observed that $b^*$ parameter showed high values mainly due to the characteristic yellowish colour that soy protein provides to the film. This parameter increased with the addition of HK, which provided a higher yellowish colour to the films. Furthermore,

HK content strengthened significantly ($P < 0.05$) the redness of the films ($a^*$), as well as the colour difference ($\Delta E^*$). Meanwhile, the employment of compression moulding as processing method increased the values of the above mentioned parameters due to the application of a higher temperature. Besides colour, transparency values of the films are also shown in **Table 2**. As can be seen, the processing method also affected the transparency of the films. Although all films were transparent (**Figure S1**), transparency values indicated that the films processed by compression moulding were more transparent, since the lower the T value, the higher the transparency [31]. However, these values did not change regardless of the amount of HK incorporated. These transparency values for compression films were similar to the values obtained for oriented polypropylene (OPP) [32]. The difference between the two methods employed in this study could be related to the use of a higher temperature by compression moulding, which favoured the denaturation of SPI and, thus, the interactions with HK, increasing the compatibility between both components.

### 3.2 Thermal properties

The thermal behaviour of the developed films was evaluated by differential scanning calorimetry (DSC) and thermogravimetric analysis (TGA) and results are presented in **Fig. 3** and **Fig. 4**, respectively. In all the DSC thermograms, one endothermic peak was detected. This peak represents the denaturation of one of the major globular proteins in SPI, β-conglycinin (7S) [33]. In the case of the films processed by casting, this thermal transition was observed around 80 ºC, but this temperature increased up to 100 ºC for compression films. It is well known that denaturation temperature of 7S globulin is strongly dependant on moisture content, thus, higher temperature values were obtained at lower moisture content [34]. As shown in **Table 1**, MC values for compression films were lower than those for casting films, in

agreement with DSC results. Additionally, the incorporation of hydrolyzed keratin caused a shift of the peak attributed to 7S globulin to higher temperatures, increasing the thermal stability of films.

As can be seen in **Fig. 4**, TGA curves showed that thermal degradation occurred in three steps. The first stage (< 100 ºC) corresponded to the loss of absorbed moisture. In this step, casting films had a weight loss of 10%, whereas the weight loss of compression films was around 5%. The point of this behaviour was a lower MC in HK-D films. The second stage, starting around 210 ºC, was related to the evaporation of the glycerol used as plasticizer. As shown in other works [35, 36], the good compatibility between protein and glycerol induced the increased of the boiling temperature of glycerol, which is 182 ºC. The third stage appeared at around 300 ºC and it was related to the thermal degradation of soy protein. It was observed that both control films (HK0-W and HK-D) experienced higher weight loss above 300 ºC than the rest of the films, suggesting that the incorporation of hydrolyzed keratin enhanced the thermal stability of the films due to a higher amount of disulfide bonds.

### 3.3. Tensile and dynamic mechanical properties

Mechanical properties of SPI-based films with different HK contents were evaluated by measuring the tensile strength (TS), elongation at break (EB) and elastic modulus (EM) and the results are set out in **Table 3**. The films prepared by compression moulding possessed an enhanced tensile strength in comparison to those processed by casting. Moreover, the incorporation of HK increased significantly ($P < 0.05$) TS values from 7.47 to 9.52 MPa for HK9-D. At the same time, compression films also exhibited higher EB values, but the addition of HK caused a decrease of EB from 131% to 94% as the HK content increased from 0 to 9 wt %. Regarding the elastic modulus, these values

were slightly higher for the films prepared by compression moulding; however, no change was observed when hydrolyzed keratin was incorporated. This change in the mechanical behaviour of the films can be related to the increase of sulphur content in film forming formulations by the incorporation of HK. As reported in the literature [37], the crosslinking by disulphide bonds in proteins is favoured at basic pH, the pH used in this work, and it is promoted by heating due to a higher degree of protein denaturation, which would explain higher TS values for compression films. Since crosslinking restricts chain mobility, increasing stress and decreasing deformation, this is in accordance with the values shown in **Table 3**.

In order to support the above mentioned effects on chain mobility, the temperature dependence of storage modulus (E'), loss modulus (E''), and loss tangent (tanδ) for SPI-based films processed with different HK contents by casting and compression is shown in **Fig. 5**. As noticed in **Fig. 5a** and **5c**, E' and E'' values were higher for films processed by compression moulding, confirming a higher thermal stability, as shown by DSC analysis. For all samples, the storage modulus was always higher than the loss modulus in the whole temperature range. However, the increase of temperature affected the thermo-mechanical behaviour of the films. As the temperature increased, the moduli values dropped sharply and a minimum value was obtained at around 45 ºC for compression films and at 30 ºC for casting films. Afterwards, and up to 80 ºC, an increase was observed. As reported in the literature, this increase in moduli can be related to the crosslinking by disulphide bonds in proteins [38]. From that temperature on, moduli values for casting films started to decrease, while those for compression films remained stable until 120 ºC.

The mechanical properties can also be related to tanδ, whose maximum defines the glass transition temperature ($T_g$). It is worth noting that the increase of $T_g$ resulted in

the increase of the resistance of the films [39]. In this context, **Fig. 5b** and **5d** showed the curves related to tanδ, where two transitions were observed. The first one, at around -45 ºC for HK0-W and -40 ºC for HK0-D, was attributed to the glass transition of glycerol ($T_{g1}$) where glycerol is loosely bound to proteins. The second one, at around 50 ºC for HK0-W and 45 ºC for HK0-D, corresponded to the glass transition of protein ($T_{g2}$) where glycerol forms a hydrogen-bound structure with proteins [40, 41]. The addition of HK contributed to the increase of $T_{g1}$ and $T_{g2}$ not only for casting films but also for compression films. This increase resulted in higher TS values and lower EB values, in accordance with the values displayed in **Table 3**.

### 3.4 Surface properties

The effect of the hydrolyzed keratin incorporation in soy protein films in terms of the chemical modification of the surface was analyzed by XPS. **Fig. S2** showed 4 different peaks related to C 1s, N 1s, Na 1s and O 1s. Sodium was related to the amount of NaOH employed in the chicken feather hydrolysis; thus, an increase of the peak intensity was observed when a higher amount of HK was added. It is known that the band frequency of C and O atoms changes depending on the interactions between the blend components, hence, a change in the intensity of the peaks was expected to occur when different processing methods were employed, as well as when different amount of hydrolyzed keratin was added [42]. In the case of HK0-W, the intensity of C 1s was higher than that related to O 1s. However, the intensity of both bands equalled with the HK incorporation. The opposite occurred for compression films, in which the peak intensity of C and O atoms was similar when no hydrolyzed keratin was incorporated.

In order to complete the information appeared in **Fig. S2**, the concentration of C 1s, O 1s and N 1s atoms on the film surface, as well as the O/C and N/C ratios, are

provided in **Table 4**. As above mentioned, the surface composition differed from one film to another depending not only on the processing method employed but also on the amount of hydrolyzed keratin incorporated. In the case of the films processed by compression moulding, the changes were more remarkable. With the addition of HK, the concentration of C increased whilst the concentration of O decreased, as shown in **Fig. S2**; therefore, the O/C ratio changed from 0.34 to 0.23 as the amount of HK increased from 0 to 9 wt %. Regarding N content, its concentration increased with the incorporation of HK content for casting films, while decreased for compression films; thus, the N/C ratio increased in the case of the films processed by casting and decreased for the ones processed by compression moulding. This fact could indicate that the content of amino groups on the film surface was higher in the films processed by casting.

C 1s peak was divided into three peaks designated as C1 (C-C and C-H), C2 (C-O and C-N) and C3 (C=O) functions. C1 indicates the hydrophobic character of the film surface, whereas C2 and C3 correspond to those functional groups which benefit the wettability of the surface [43, 44]. As can be seen in **Table 5**, C1 content was higher for compression films. Moreover, C1 values increased with HK incorporation, increasing the hydrophobic character of the films, as confirmed by WCA values. This fact could evidence the reorganization of the chemical groups at the surface upon hydrolyzed keratin incorporation which might promote the change in surface hydrophobicity.

In order to provide further information about the surface properties of the films, the assessment of gloss was carried out. In fact, gloss is directly related to the surface roughness, being lower when surface is rougher [45]. **Table 6** shows gloss values for the films with different HK contents processed by casting and compression. Gloss values higher than 70 º were taken as frame of reference to define the film as a glossy

material with smooth surface [46]. Films prepared by compression moulding showed higher values of gloss than those prepared by casting due to a smoother surface, in accordance with SEM images shown in **Figure S3**, as a consequence of the application of pressure during processing. Furthermore, the incorporation of hydrolyzed keratin into the films decreased significantly ($P < 0.05$) the gloss values. For instance, with the addition of 9 wt % HK, the gloss values of casting films decreased from 10.60 º to 4.40 º and, in the case of compression films, from 33.60 º to 23.40. These results indicated that the films processed with HK were glossier, in agreement with their smoother surface observed in **Figure S3**.

## 4. Conclusions

Soy protein-based films reinforced with hydrolyzed feather keratin and processed by casting and compression moulding were successfully manufactured due to the good compatibility among the components, resulting in transparent films. Films processed by compression achieved better mechanical properties in terms of tensile strength, which increased with the incorporation of hydrolyzed keratin. Interestingly, it was observed that the water uptake of the films remained constant after 24 h, indicating a high stability and structural integrity of the manufactured films. Consequently, the incorporation of hydrolyzed keratin into soy protein formulations opens up new opportunities to develop sustainable films with higher stability.

## Acknowledgments

Authors thank the University of the Basque Country UPV/EHU (PPG17/18 research group) and the Provincial Council of Gipuzkoa (Exp. 81/17) for their financial support. Also thanks are due to Advanced Research Facilities (SGIker) from the

UPV/EHU. Tania Garrido thanks Euskara Errektoreordetza (UPV/EHU) for her fellowship.

**References**

[1] A. Etxabide, J. Uranga, P. Guerrero, K. de la Caba, Development of active gelatin films by means of valorisation of food processing waste: A review, Food Hydrocolloids 68 (2017) 192-198.

[2] I. Leceta, J. Uranga, P. Arana, S. Cabezudo, K. de la Caba, P. Guerrero, Valorisation of fishery industry wastes to manufacture sustainable packaging films: modelling moisture-sorption behaviour, J Cleaner Prod 91 (2015) 36-42.

[3] T. Väisänen, A. Haapala, R. Lappalainen, L. Tomppo L, Utilization of agricultural and forest industry waste and residues in natural fiber-polymer composites: A review, Waste Manage 54 (2016) 62-73.

[4] C.R. Alvarez-Chávez, S. Edwards, R. Moure-Eraso, K. Geiser, Sustainability of bio-based plastics: general comparative analysis and recommendations for improvement, J Cleaner Prod 23 (2012) 47-56.

[5] A. Bhatnagar, F. Kaczala, W. Hogland, M. Marques, C.A. Paraskeva, V.G. Papadakis, M. Sillanpää, Valorization of solid waste products from olive oil industry as potential adsorbents for water pollution control: A review, Environ Sci Pollut Res 21 (2014) 268-298.

[6] W. Liu, T. Liu, H. Liu, J. Xin, J. Zhang, Z.K. Muhidinov, L. Liu, Properties of poly (butylenes adipate-co-terephtalate) and sunflower head residue biocomposites, J Appl Polym Sci 134 (2017) 44644-44652.

[7] J. Uranga, I. Leceta, A. Etxabide, P. Guerrero, K. de la Caba, Cross-linking of fish gelatins to develop sustainable films with enhanced properties, Eur Polym J 78 (2016) 82-90.

[8] Y. Xu, A. Scales, K. Jordan, C. Kim, E. Sismour, Starch nanocomposite films incorporating grape pomace extract and cellulose nanocrystal, J Appl Polym Sci 134 (2017) 44438-44447.

[9] S.I.N. Ayuttaya, S. Tanpichai, J. Wootthikanokkhan, Keratin extracted from chicken feather waste: Extraction, preparation and structural characterization of the keratin and keratin/biopolymer films and electrospuns, J Polym Environ 23 (2015) 506-516.

[10] L.T. Zhou, G. Yang, X.X. Yang, Preparation of regenerated keratin sponge from waste feathers by a simple method and its potential use for oil adsorption, Environ Sci Pollut Res 21 (2014) 5730-5736.

[11] S. Al-Asheh, F. Banat, D. Al-Rousan, Beneficial reuse of chicken feathers in removal of heavy metals from wastewater, J Cleaner Prod 11 (2003) 321-326.

[12] M.J. Fabra, P. Pardo, M. Martínez-Sanz, A. Lopez-Rubio, J.M. Lagarón, Combining polyhydroxyalkanoates with nanokeratin to develop novel biopakaging structures, J Appl Polym Sci 133 (2016) 42695-42707.

[13] T. Tesfaye, B. Sithole, D. Ramjugernath, V. Chunilall, Valorisation of chicken feathers: Characterisation of physical properties and morphological structure, J Cleaner Prod 149 (2017) 349-365.

[14] J. Wang, S. Hao, T. Luo, Z. Cheng, W. Li, F. Gao, T. Guo, Y. Gong, B. Wang, Feather keratin hydrogel for wound repair: Preparation, healing effect and biocompatibility evaluation, Colloids Surf B 149 (2017) 341-350.

[15] Y. Dou, X. Huang, B. Zhang, M. He, G. Yin, Y. Cui, Preparation and characterization of a dialdehyde starch crosslinked feather keratin film for food packaging applications, RSC Adv 5 (2015) 27168-27174.

[16] X.C. Yin, F.Y. Li, Y.F. He, Y. Wang, R.M. Wang, Study on effective ectraction of chicken feather keratins and their films for controlling drug release, Biomater Sci 1 (2013) 528-536.

[17] A.J. Poole, J.S. Church, The effects of physical and chemical treatments on $Na_2S$ produced feather keratin films. Int J Biol Macromol 73, (2015) 99-108.

[18] F. Song, D.L. Tang, X.L. Wang, Y.Z. Wang YZ, Biodegradable soy protein isolate-based materials: A review, Biomacromolecules 12 (2011) 3369-3380.

[19] K. Nishinari, Y. Fang, S. Guo, G.O. Phillips, Soy protein: A review on composition, aggregation and emulsification, Food Hydrocolloids 39 (2014) 301-318.

[20] V.M. Hernandez-Izquierdo, J.M. Krochta. Thermoplastic processing of proteins for film formation: A review. J Food Sci 73 (2008) 30-39.

[21] T. Garrido, I. Leceta, S. Cabezudo, P. Guerrero, K. de la Caba, Tailoring soy protein film properties by selecting casting or compression as processing methods, Eur Polym J 85 (2916) 499-507.

[22] A. Jerez, P. Partal, I. Martínez, C. Gallegos, A. Guerrero, Protein-based bioplastics: Effect of thermo-mechanical processing. Rheol Acta 46 (2007) 711-720.

[23] J. Gómez-Estaca, R. Gavara, R. Catalá, P. Hernández-Muñoz, The potential of proteins for producing food packaging materials: A review. Packag Technol Sci 29 (2016) 203-224.

[24] B. Cuq, N. Gontard, J.L. Cuq, S. Guilbert, Functional properties of myofibrillar protein-based biopackaging as affected by film thickness. J Food Sci 61 (1996) 580-584.

[25] ASTM E96-00, Standard test methods for water vapour transmission of materials, In: Annual book of ASTM Standards. American Society for Testing and Materials, Philadelphia: 2000.

[26] ASTM D638-03, Standard test method for tensile properties of plastics, In: Annual book of ASTM Standards, American Society for Testing and Materials, Philadelphia: 2003.

[27] ASTM D523-14, Standard test method for specular gloss, In: Annual book of ASTM Standards, American Society for Testing and Materials. Philadelphia: 2014.

[28] C.E. Tanase, J. Spiridon, PLA/chitosan/keratin composites for biomedical applications, Mater Sci Eng C 40 (2014) 242-247.

[29] Y.P. Timilsena, R. Adhikari, C.J. Barrow, B. Adhikari, Physicochemical and functional properties of protein isolate produced from Australian chia seeds, Food Chem 212 (2016) 648-656.

[30] T. Karbowiak, F. Debeaufort, D. Champion, A. Voilley, Wetting properties at the surface of iota-carrageenan-based edible films, J Colloid Interface Sci 294 (2006) 400-410.

[31] A. Nawab, F. Alam, M.A. Haq, Z. Lutfi, A. Hasnain, Mango kernel starch-gum composite films: Physical, mechanical and barrier properties, Int J Biol Macromol 98 (2017) 869-876.

[32] P. Guerrero, Z.A. Nur Hanani, J.P. Kerry, K. de la Caba, Characterization of soy protein-based films prepared with acids and oils by compression. J Food Eng 107 (2011) 41-49.

[33] G. Denavi, D.R. Tapia-Blácido, M.C. Añón, P.J.A. Sobral, A.N. Mauri, F.C. Menegalli, Effects of drying conditions on some physical properties of soy protein films, J Food Eng 90 (2009) 341-349.

[34] R.R. Koshy, S.K. Mary, L.A. Pothan, S. Thomas, Soy protein-and starch-based green composites/nanocomposites: Preparation, properties, and applications, In: Thakur VK and Thakur MK editors, Eco-friendly polymer nanocomposites India: Springer (2015) 433-467.

[35] X. Mo, X. Sun, Plastification of soy protein polymer by polyol-based plasticizers, J Am Oil Chem Soc 79 (2002) 197-202.

[36] H. Tian, W. Wu, G. Guo, B. Gaolum, Q. Jia, A. Xiang, Microstructure and properties of glycerol plasticized soy protein plastics containing castor oil, J Food Eng 109 (2012) 496-500.

[37] R.W. Visschers, H.H.J. de Jongh, Disulphide bond formation in food protein aggregation and gelation. Biotechnol Adv 23 (2005) 75-80.

[38] L. Fernández-Espada, C. Bengoechea, F. Cordobés, A. Guerrero, Protein/glycerol blends and injection-molded bioplastic matrices: Soybean versus egg albumen. J Appl Polym Sci 133 (2016) 43524-43534.

[39] G.P.R. Moore, S.M. Martelli, C. Gandolfo, P.J.A. Sobral, J.B. Laurindo, Influence of the glycerol concentration on some physical properties of feather keratin films, Food Hydrocolloids 20 (2006) 975-982.

[40] P. Chen, L. Zhang, New evidences of glass transitions and microstructures of soy protein plasticized with glycerol, Macromol Biosci 5 (2005) 237-245.

[41] Y. Dou, B. Zhang, M. He, G. Yin, Y. Cui, The structure, tensile properties and water resistance of hydrolyzed feather keratin-based bioplastics, Chin J Chem Eng 24 (2016) 415-420.

[42] P. Guerrero, T. Garrido, I. Leceta, K. de la Caba, Films based on proteins and polysaccharides, Eur Polym J 49 (2013) 3713-3721.

[43] X. Zhao, J. Chen, Q. Zhu, F. Du, Q. Ao, J. Liu, Surface characterization of 7S and 11S globulin by X-ray photoelectron spectroscopy and scanning electron microscopy, Colloids Surf B 86 (2011) 260-266.

[44] Y. Li, F. Chen, L. Zhan, Y. Yao, Effect of surface changes of soy protein materials on water resistance, Mater Lett 149 (2015) 120-122.

[45] G. Ward, A. Nussinovitch, Characterizing the gloss properties of hydrocolloid films, Food Hydrocolloids 11 (2017) 357-365.

[46] T.A. Trezza, J.M. Krochta, The gloss of edible coatings as affected by surfactants, lipids, relative humidity and time, J Food Sci 65 (2000) 658-662.

**Figure captions**

**Fig. 1.** Water uptake of SPI films processed by casting (W) and compression (D) as a function of HK content.

**Fig. 2.** Water contact angle values (º) of the control films and the films with 9 wt % HK processed by casting (W) and compression (D) and recorded at 0, 5 and 10.

**Fig. 3.** DSC thermograms of SPI films processed by casting (W) and compression (D) as a function of HK content.

**Fig. 4.** TGA and DTG curves of SPI films processed by casting (W) and compression (D) as a function of HK content**.**

**Fig. 5.** Temperature dependence of the storage modulus (E'), loss modulus (E'') and loss tangent (tanδ) curves for SPI films processed by casting (**a** and **b**) and compression (**c** and **d**) as a function of HK content.

**Supplementary figures**

**Fig. S1.** Images of the films containing 0 and 9 wt % of hydrolyzed keratin processed by casting (HK0-W and HK9-W) and compression moulding (HK0-D and HK9-D).

**Fig. S2.** XPS survey spectra of SPI-based films processed by casting and compression as a function of HK content.

**Fig. S3.** SEM micrographs of the surface of those films containing 0 and 9 wt % of hydrolyzed keratin processed by casting (HK0-W and HK9-W) and compression moulding (HK0-D and HK9-D).

**Table Captions**

**Table 1.** Moisture content (MC), total soluble matter (TSM), and water vapour permeability (WVP) of the films processed by casting (W) and compression (D) as a function of HK content**.**

**Table 2.** Colour ($L^*$, $a^*$, $b^*$ and $\Delta E^*$) and transparency (T) values of SPI films processed by casting (W) and compression (D) as a function of HK content**.**

**Table 3.** Tensile strength (TS), elongation at break (EB) and elastic modulus (EM) of SPI films processed by casting (W) and compression (D) as a function of HK content**.**

**Table 4.** Compositional information by XPS of the SPI-based films processed by casting (W) and compression (D) as a function of HK content**.**

**Table 5.** Content of C1, C2 and C3 determined by XPS for SPI-based films processed by casting (W) and compression (D) as a function of HK content**.**

**Table 6.** Gloss values of the SPI-based films processed by casting (W) and compression (D) as a function of HK content**.**

**Fig. 1.**

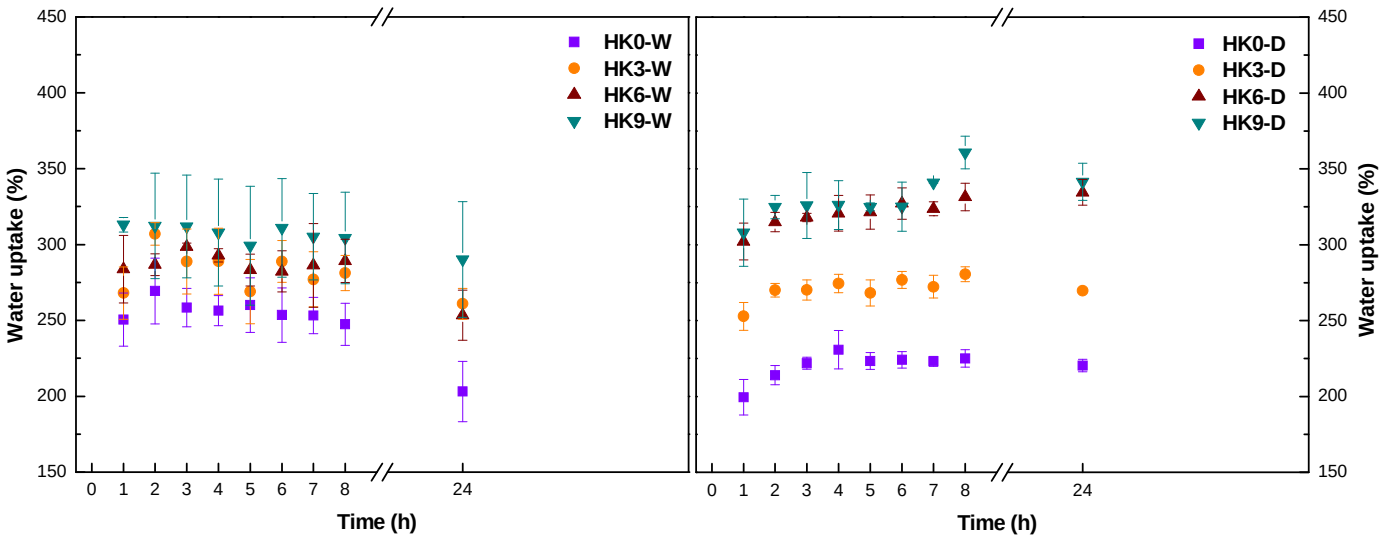
Water uptake (%)
Time (h)
HK0-W
HK3-W
HK6-W
HK9-W
HK0-D
HK3-D
HK6-D
HK9-D
150
200
250
300
350
400
450
0
1
2
3
4
5
6
7
8
24

**Fig. 2.**

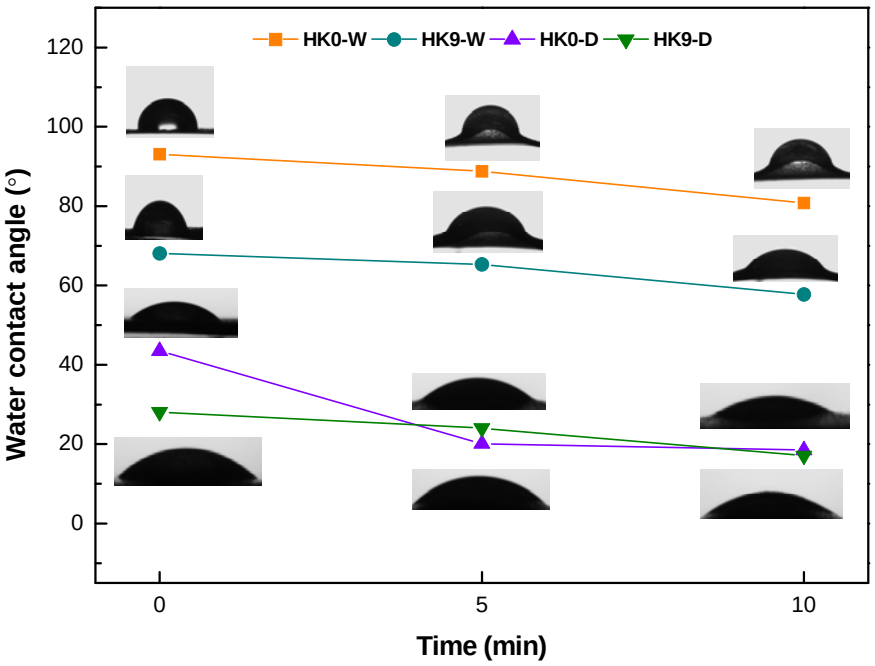
HK0-W
HK9-W
HK0-D
HK9-D
Water contact angle (°)
120
100
80
60
40
20
0
0
5
10
Time (min)

**Fig. 3.**

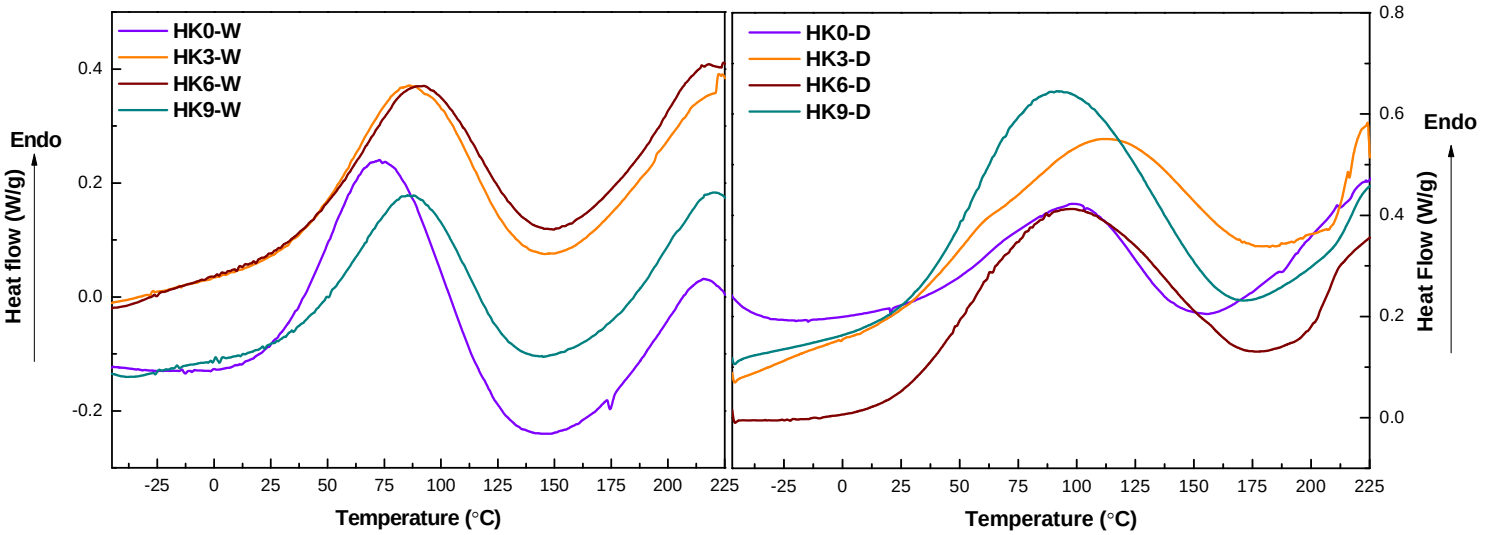
HK0-W
HK3-W
HK6-W
HK9-W
Endo
Heat flow (W/g)
Temperature (°C)
HK0-D
HK3-D
HK6-D
HK9-D
Endo
Heat Flow (W/g)
Temperature (°C)

Fig. 4

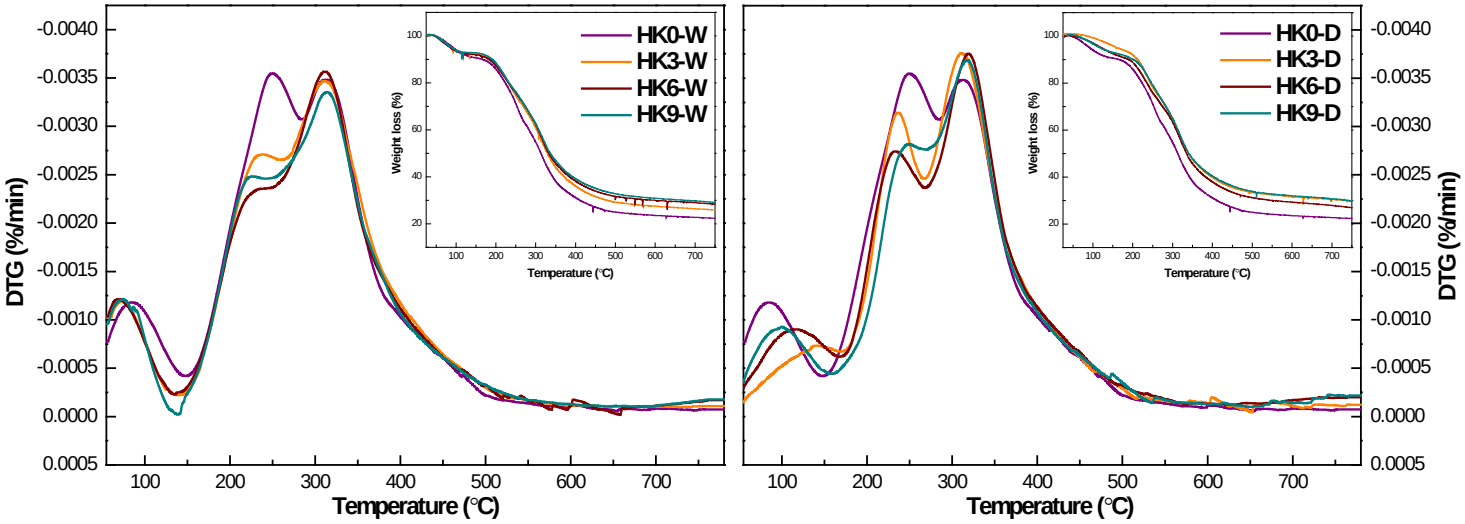
DTG (%/min)
Temperature (°C)
HK0-W
HK3-W
HK6-W
HK9-W
Weight loss (%)
HK0-D
HK3-D
HK6-D
HK9-D

**Fig. 5.**

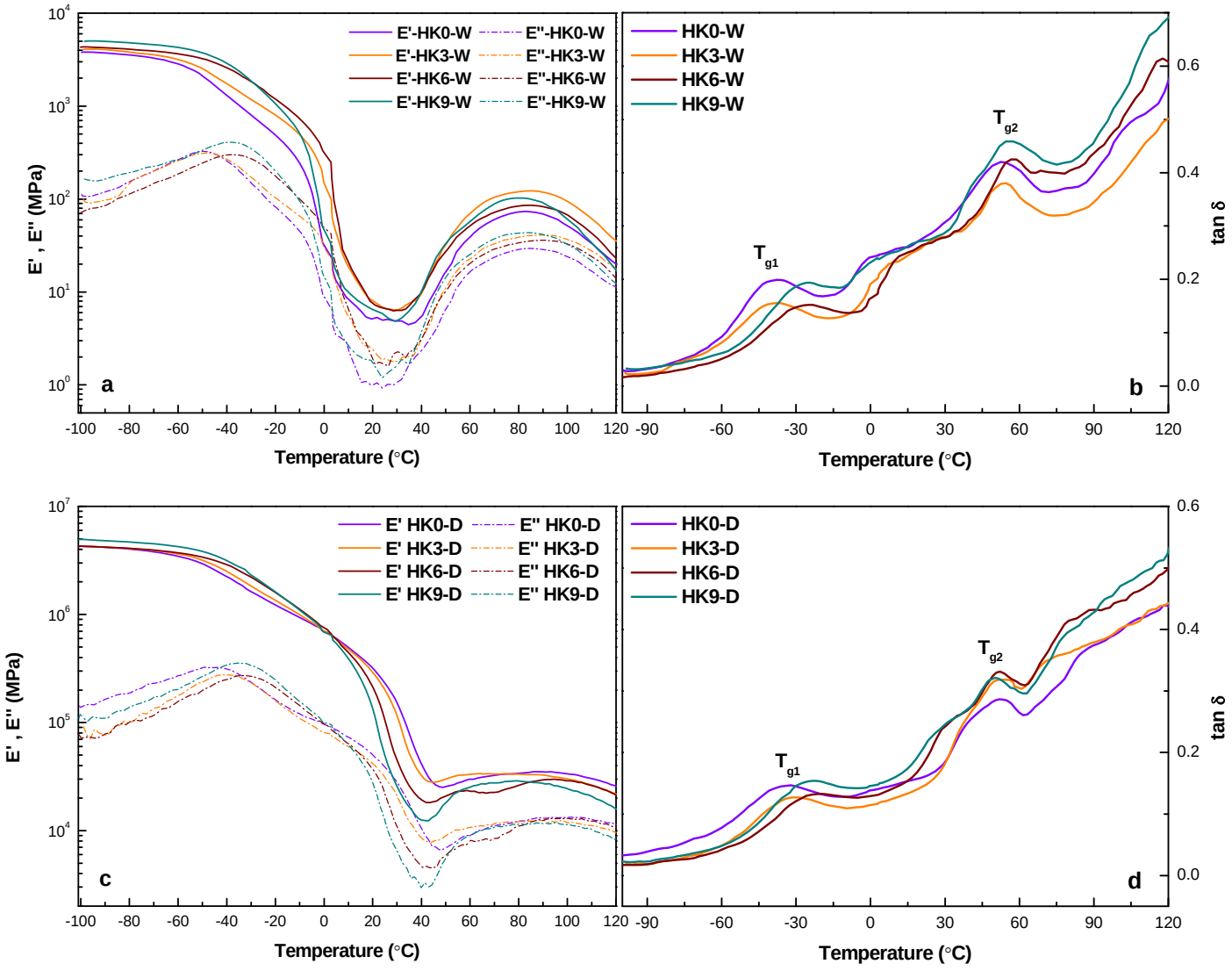
E'-HK0-W
E''-HK0-W
E'-HK3-W
E''-HK3-W
E'-HK6-W
E''-HK6-W
E'-HK9-W
E''-HK9-W
E' , E'' (MPa)
Temperature (°C)
a
HK0-W
HK3-W
HK6-W
HK9-W
$T_{g1}$
$T_{g2}$
tan δ
b
E' HK0-D
E'' HK0-D
E' HK3-D
E'' HK3-D
E' HK6-D
E'' HK6-D
E' HK9-D
E'' HK9-D
c
HK0-D
HK3-D
HK6-D
HK9-D
d

**Figure S1**

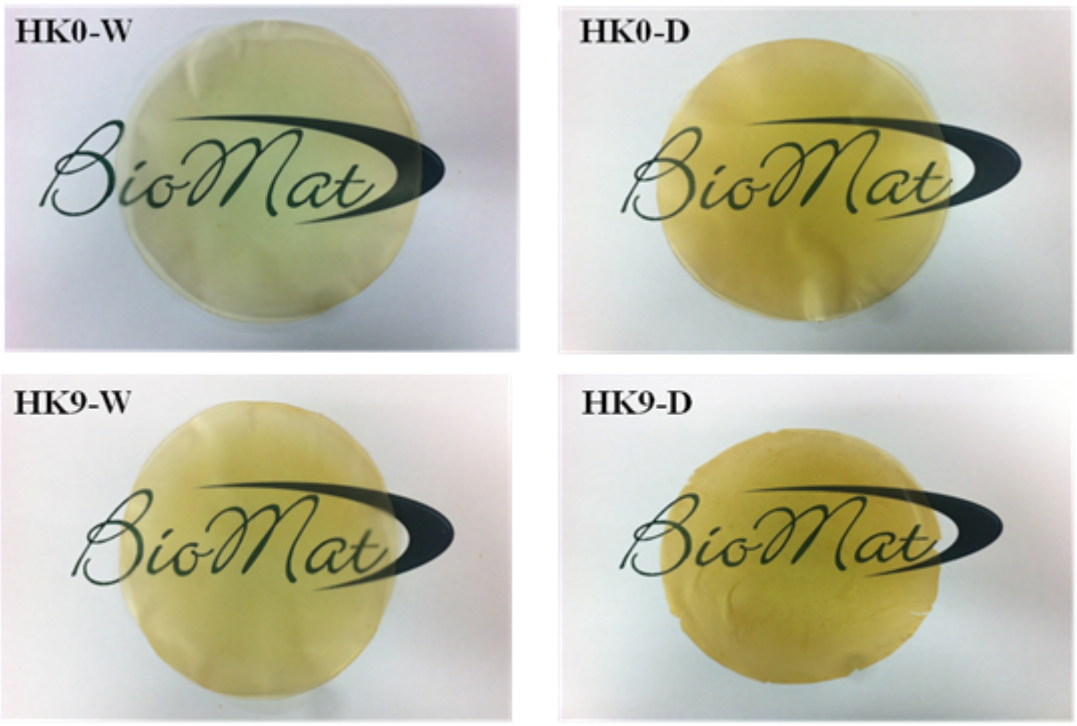

**Figure S2**

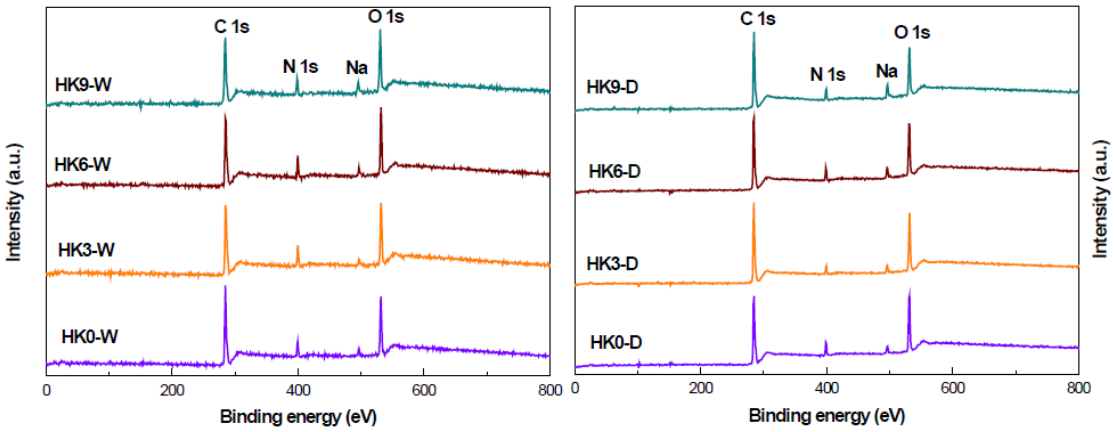
C 1s
O 1s
N 1s
Na
HK9-W
HK6-W
HK3-W
HK0-W
HK9-D
HK6-D
HK3-D
HK0-D
Intensity (a.u.)
Binding energy (eV)
0
200
400
600
800

**Figure S3**

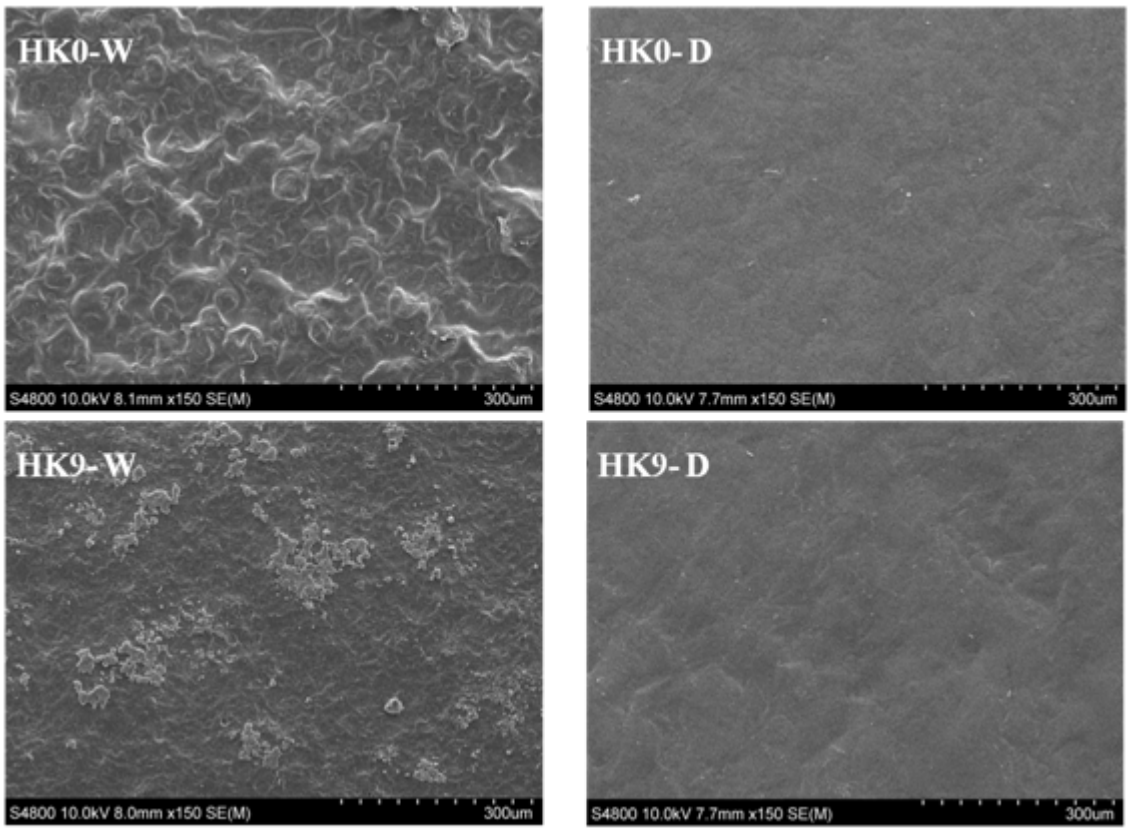
HK0-W
S4800 10.0kV 8.1mm x150 SE(M)
300um
HK0- D
S4800 10.0kV 7.7mm x150 SE(M)
300um
HK9-W
S4800 10.0kV 8.0mm x150 SE(M)
300um
HK9- D
S4800 10.0kV 7.7mm x150 SE(M)
300um

**Table 1.** Moisture content (MC), total soluble matter (TSM), and water vapour permeability (WVP) of the films processed by casting (W) and compression (D) as a function of HK content.

| Film | MC (%) | TSM (%) | WVP ($10^{-12}$ g cm/cm$^2$ s Pa) |
|---|---|---|---|
| **HK0-W** | 17.45 ± 0.77$^{a}$ | 29.06 ± 0.92$^{a}$ | 3.74 ± 0.24$^{a}$ |
| **HK3-W** | 17.32 ± 1.57$^{a}$ | 31.13 ± 3.02$^{a}$ | 3.45 ± 0.34$^{a}$ |
| **HK6-W** | 17.03 ± 0.43$^{a}$ | 32.11 ± 3.74$^{ab}$ | 3.55 ± 0.17$^{a}$ |
| **HK9-W** | 15.84 ± 1.44$^{a}$ | 36.87 ± 2.47$^{b}$ | 3.54 ± 0.47$^{a}$ |
| **HK0-D** | 11.58 ± 0.11$^{b}$ | 28.57 ± 0.38$^{a}$ | 5.62 ± 0.14 $^{a}$ |
| **HK3-D** | 11.07 ± 0.02$^{a}$ | 31.02 ± 0.29$^{b}$ | 5.82 ± 0.39$^{b}$ |
| **HK6-D** | 11.67 ± 0.12$^{b}$ | 33.03 ± 0.14$^{c}$ | 6.74 ± 0.15$^{b}$ |
| **HK9-D** | 12.88 ± 0.25$^{c}$ | 34.74 ± 0.04$^{d}$ | 6.76 ± 0.33$^{b}$ |

$^{a\text{-}d}$Two means followed by the same letter in the same column and in the same section are not significantly ($P > 0.05$) different through the Duncan's multiple range test.

**Table 2.** Colour (L*, a*, b* and ΔE*) and transparency (T) values of SPI films processed by casting (W) and compression (D) as a function of HK content.

| Film | L* | a* | b* | ΔE* | T |
|---|---|---|---|---|---|
| **HK0-W** | 90.78 ± 0.37[a] | -1.26 ± 0.06[a] | 20.98 ± 0.27[a] | | 8.71 |
| **HK3-W** | 86.03 ± 0.37[b] | 1.09 ± 0.15[b] | 27.84 ± 0.75[b] | 8.67 ± 0.82[a] | 7.81 |
| **HK6-W** | 80.07 ± 0.32[c] | 4.26 ± 0.17[c] | 36.70 ± 0.49[c] | 19.81 ± 0.54[b] | 7.02 |
| **HK9-W** | 76.43 ± 0.20[d] | 6.36 ± 0.10[d] | 40.11 ± 0.14[d] | 25.17 ± 0.25[c] | 6.83 |
| **HK0-D** | 78.94 ± 0.80[a] | 2.84 ± 0.60[a] | 46.53 ± 1.20[a] | | 1.16 |
| **HK3-D** | 71.19 ± 0.79[b] | 9.87 ± 0.28[b] | 53.37 ± 0.72[b] | 12.54 ± 0.88[a] | 1.17 |
| **HK6-D** | 68.11 ± 0.83[c] | 11.72 ± 0.42[c] | 52.67 ± 0.84[bc] | 15.35 ± 0.52[b] | 1.25 |
| **HK9-D** | 66.65 ± 0.24[d] | 14.63 ± 0.36[d] | 54.42 ± 0.37[c] | 18.79 ± 0.37[c] | 1.35 |

[a-d]Two means followed by the same letter in the same column and in the same section are not significantly (P > 0.05) different through the Duncan's multiple range test.

**Table 3.** Tensile strength (TS), elongation at break (EB) and elastic modulus (EM) of SPI films processed by casting (W) and compression (D) as a function of HK content.

| Film | TS (MPa) | EB (%) | EM (MPa) |
|---|---|---|---|
| **HK0-W** | $4.03 \pm 0.14^{a}$ | $103.92 \pm 10.10^{a}$ | $113.79 \pm 4.42^{a}$ |
| **HK3-W** | $4.83 \pm 0.27^{b}$ | $97.80 \pm 7.44^{a}$ | $104.25 \pm 13.19^{a}$ |
| **HK6-W** | $5.12 \pm 0.66^{bc}$ | $98.03 \pm 8.49^{a}$ | $99.28 \pm 10.06^{a}$ |
| **HK9-W** | $5.59 \pm 0.53^{c}$ | $97.68 \pm 8.99^{a}$ | $97.29 \pm 10.87^{a}$ |
| **HK0-D** | $7.47 \pm 1.01^{a}$ | $131.37 \pm 7.83^{a}$ | $112.68 \pm 9.62^{a}$ |
| **HK3-D** | $8.09 \pm 0.83^{ab}$ | $110.44 \pm 8.23^{b}$ | $109.40 \pm 10.04^{a}$ |
| **HK6-D** | $8.92 \pm 0.56^{bc}$ | $101.34 \pm 2.65^{bc}$ | $104.19 \pm 5.99^{a}$ |
| **HK9-D** | $9.52 \pm 0.90^{c}$ | $94.27 \pm 9.78^{c}$ | $101.58 \pm 8.95^{a}$ |

$^{a\text{-}c}$Two means followed by the same letter in the same column and in the same section are not significantly ($P > 0.05$) different through the Duncan's multiple range test.

**Table 4.** Compositional information by XPS of the SPI-based films processed by casting (W) and compression (D) as a function of HK content.

| Film | C (%) | O (%) | N (%) | O/C | N/C |
|---|---|---|---|---|---|
| **HK0-W** | 72.29 | 20.91 | 6.45 | 0.29 | 0.09 |
| **HK3-W** | 68.81 | 21.61 | 9.26 | 0.31 | 0.13 |
| **HK6-W** | 70.22 | 21.09 | 8.16 | 0.30 | 0.12 |
| **HK9-W** | 70.47 | 20.86 | 8.03 | 0.29 | 0.11 |
| **HK0-D** | 69.08 | 23.41 | 6.95 | 0.34 | 0.10 |
| **HK3-D** | 72.16 | 22.89 | 4.33 | 0.32 | 0.06 |
| **HK6-D** | 73.88 | 19.80 | 5.49 | 0.27 | 0.07 |
| **HK9-D** | 75.85 | 17.26 | 5.14 | 0.23 | 0.07 |

**Table 5.** Content of C1, C2 and C3 determined by XPS for SPI-based films processed by casting (W) and compression (D) as a function of HK content.

| Film | C1 (%) | C2 (%) | C3 (%) |
|---|---|---|---|
| **HK0-W** | 52.82 | 12.66 | 6.78 |
| **HK3-W** | 45.78 | 13.31 | 9.69 |
| **HK6-W** | 46.76 | 15.43 | 8.02 |
| **HK9-W** | 48.68 | 14.08 | 7.71 |
| **HK0-D** | 44.75 | 16.61 | 7.72 |
| **HK3-D** | 50.65 | 15.96 | 5.55 |
| **HK6-D** | 51.91 | 15.20 | 6.76 |
| **HK9-D** | 55.09 | 14.49 | 6.27 |

**Table 6.** Gloss values of the SPI-based films processed by casting (W) and compression (D) as a function of HK content.

| Film | Gloss (º) |
|---|---|
| **HK0-W** | 10.60 ± 0.11[a] |
| **HK3-W** | 8.20 ± 0.05[b] |
| **HK6-W** | 5.50 ± 0.04[c] |
| **HK9-W** | 4.40 ± 0.11[d] |
| **HK0-D** | 33.60 ± 1.23[a] |
| **HK3-D** | 6.60 ± 0.36[d] |
| **HK6-D** | 10.60 ± 2.61[c] |
| **HK9-D** | 23.40 ± 1.17[b] |

[a-d]Two means followed by the same letter in the same column and in the same section are not significantly (P > 0.05) different through the Duncan´s multiple range test.